Submitted: 31 October, 2023 Accepted: 11 January, 2024 Published: 03 September, 2024 DOI:10.22514/jocpd.2024.115

ORIGINAL RESEARCH

Journal of Clinical Pediatric Dentistry

Cytotoxicity of two fluoride-releasing adhesive tapes

Seo-Rin Jeong[1,†], Yong Kwon Chae[2,†], Ok Hyung Nam[2,3], Tae-Young Park[4], Jonghyun Shin[5], Myeong-Kwan Jih[6,*]

[1]Department of Orthodontics, School of Dentistry, Chosun University, 61452 Gwangju, Republic of Korea
[2]Department of Pediatric Dentistry, Kyung Hee University, College of Dentistry, Kyung Hee University Medical Center, 02447 Seoul, Republic of Korea
[3]Department of Pediatric Dentistry, School of Dentistry, Kyung Hee University, 02447 Seoul, Republic of Korea
[4]Department of Conservative Dentistry, School of Dentistry, Chosun University, 61452 Gwangju, Republic of Korea
[5]Department of Pediatric Dentistry, School of Dentistry, Pusan National University, 50612 Yangsan, Republic of Korea
[6]Department of Pediatric Dentistry, School of Dentistry, Chosun University, 61452 Gwangju, Republic of Korea

***Correspondence**
mdenti@chosun.ac.kr
(Myeong-Kwan Jih)

† These authors contributed equally.

Abstract

Sodium fluoride-polyvinyl alcohol (NaF-PVA) tape was developed to deliver fluoride to teeth by adding fluoride to polymer tape. Previous studies have demonstrated that tapes are effective and have antimicrobial properties. This study aimed to evaluate the cytotoxicity of two fluoride-releasing adhesive tapes. We investigated two polyvinyl alcohol (PVA) tapes: (i) a fluoride-PVA (F-PVA) tape, and (ii) a pullulan-incorporated F-PVA (PF-PVA) tape. The cytotoxicity test was conducted on human gingival fibroblasts (HGF) and human periodontal ligament (PDL) cells. Using an adhesive tape containing fluoride, we performed the 3-(4,5-dimethylthiazol-2-yl)-2,5-diphenyltetrazolium bromide (MTT) assay on these cells. Genetic analysis of the cells was performed to conduct a stability test on humans. In the MTT assay, PF-PVA had 66% greater cytotoxicity than control by PDL and 69% by HGF. F-PVA showed less cytotoxicity than PF-PVA by 29% in PDL and 33% in HGF. Gene ontology (GO) analysis and gene set enrichment analysis (GSEA) were performed as gene expression analyses. GO analysis indicated that PF-PVA displayed more expression changes of genes related to cytotoxicity than F-PVA. In addition, GSEA found more inflammatory response associations in PF-PVA than in F-PVA. MTT and genetic testing yielded comparable results.

Keywords

Fluoride; Polyvinyl alcohol tape; Pullulan; Cytotoxicity

1. Introduction

Modern dentistry focuses on preventative dentistry. In particular, non-invasive management of early carious lesions is possible through remineralization, where control and adjustment of demineralization and remineralization are considered keys to preventing dental caries [1, 2]. To control and adjust demineralization and remineralization of teeth, fluoride is widely used [3, 4].

Fluoride is considered the most ideal remineralization agent to date [5]. Professional fluoridation began with fluoride solution application in 1943, and fluoride varnish is now the most widely used [6]. Fluoride varnish is now the most popular preventive fluoridation method available to professionals in the United States after the US Food and Drug Administration (FDA) approval in 1994 [7]. However, most fluoride varnishes contain rosin, which has an unpleasant flavor and texture that some children may find objectionable and results in temporary staining of teeth [8]. Additionally, fluoride varnishes are easily removed with saliva and do not provide a durable fluoride solution.

The ideal fluoride delivery vehicle should be easily adaptable, efficient and allow sustained fluoride release [9–11]. To achieve these conditions, fluoride-polyvinyl alcohol (F-PVA) tape was developed by supplementing a polymer-based substrate with nanosized fluoride particles. F-PVA tape covers all teeth in both arches with about 33% fluoride contained in fluoride varnish [12]. By adding fluoride to PVA, a polymeric agent and bonding it to the teeth, adequate fluoride levels in the oral cavity are maintained for a long time. Fluoride-containing films are colorless, odorless, tasteless, biocompatible and anti-decalcifying [12]. Also, F-PVA tapes are efficacious in treating dental hypersensitivity compared with fluoride varnish [13].

Previously, we developed a fluoride adhesive film coated with sodium fluoride on a polymer-based substrate [12]. A new fluoride delivery system was developed using fluoride-PVA (F-PVA) tape and pullulan incorporated F-PVA (PF-PVA) tape [14]. The superior antimicrobial efficacy of F-PVA against S. Mutans compared to PF-PVA with added pullulan was confirmed. These previous findings suggested that fluoride use in dental caries prevention may reduce PF-PVA's antimicrobial efficacy while improving adhesion and user-friendliness.

Commercialization of fluoride adhesive films requires improved remineralization effects and stability. However, previous studies on fluoride adhesive films have primarily focused on remineralization or dental caries prevention. The lack of bio-stability studies has hampered fluoride adhesive films commercialization [12, 15, 16].

To assess fluoride adhesive film safety, this study conducted

a cytotoxicity experiment. Considering the potential of fluoride adhesive films to come in contact with gingiva or periodontal ligament, cytotoxicity on human gingival fibroblast (HGF) and human periodontal ligament (PDL) was tested via 3-(4,5-dimethylthiazol-2-yl)-2,5-diphenyltetrazolium bromide (MTT) assay and genetic analysis. As described above, cytotoxicity was compared between previously developed fluoride adhesive film and newly developed double layer fluoride adhesive film supplemented with pullulan.

The study aimed to determine the difference in the toxicity of PF-PVA, which is designed to increase adhesion, compared to F-PVA, a more stable formulation. We hypothesized that there were no differences in cytotoxicity between the investigated tape groups.

2. Materials and methods

2.1 Preparation of tapes

The experimental samples were divided as follows:

(i) Control group: PVA tape with no fluoride supplementation

(ii) F-PVA group: PVA tape with 5% NaF

(iii) PF-PVA group: F-PVA tape with a pullulan layer

All tapes were prepared according to a method described in [14].

2.1.1 Preparation of F-PVA tape

PVA (10 g) and polyacrylic acid (5 g) were mixed and stirred in 85 g of distilled water at 85 ℃ for 2 h. Polyethylene glycol (3 g) and NaF (0.95 g) were added gradually and stirred at 85 ℃ for 2 h. The mixture was then poured onto a glass plate and uniformly spread in width (80 μm) using an applicator, and then dried at 40 ℃ for 24 h.

2.1.2 Preparation of PF-PVA tape

A mixture incorporating 10 wt% polyurethane powder and 2 wt% polyethylene glycol (P3015, Sigma-Aldrich, St. Louis, MO, USA) as a solvent was prepared, and stirred for 2 h. Subsequently, a 40 μm polyurethane adhesive film solution was applied to dried F-PVA tape, and an additional layer of 40 μm, resulting in a total thickness of 80 μm, was created using an applicator.

2.2 MTT assay

To assess the cytotoxicity of fluoride adhesive film on oral cells, cell viability was observed by MTT assay, as in previous studies [17]. MTT storage solution was prepared by dissolving 5 mg/mL of MTT in sterilized phosphate buffered saline (PBS). We prepared fresh MTT solution by mixing 1 mL of MTT storage solution and 9 mL of sterilized PBS. HGF and PDL cells (1×10^4/well) were seeded in 12-well plates and incubated in a CO_2 incubator for 48 h at 37 ℃. After removing the fluoride adhesive film from the plate, cells were treated with 200 mL of MTT solution and incubated for an additional 2 h. Subsequently, 200 mL of dimethyl sulfoxide (0231, DMSO, Amresco, Solon, OH, USA) was added. The solution was transferred to a 96-wall plate and a microtiter reader (SPECTROstar Nano, BMG Labtech, Ortenberg, Germany) was used for observation at 540 nm. Three independent experiments were performed on each group. According to the international organization for standardization (ISO) 10993-5 (Biological evaluation of medical devices—part 5: tests for *in vitro* cytotoxicity), a biomaterial was considered cytotoxic if it induced a 30% or greater reduction in cell viability compared to the control.

2.3 RNA sequencing

To investigate the effects of fluoride adhesive films on gene expression by oral cells, RNA sequencing was performed on HGF and PDL cells. We seeded HGF and PDL cells (1×10^4/well) in 12-well plates and incubated in a CO_2 incubator for 48 h at 37 ℃. The cells were allowed to be in contact with the adhesive films for 5 h. The films and medium were removed and the plate was washed twice with sterilized PBS. RNA sequencing was performed (EBIOGEN, Seoul, Korea) following preparation of RNA samples with the RNeasy Plus Mini kit (74134, Qiagen, Düsseldorf, Germany) according to the manufacturer's protocol.

We tested the quality of mRNA extracted from HGF and PDL cells using an ND-2000 spectrophotometer (Thermo Inc., Waltham, DE, USA), then the library was created through a cloning process by synthesizing cDNA using QuantSeq 3′ mRNA-Seq Library Prep Kit (Lexogen, Inc., Vienna, Austria). Nextseq500 (Illumina, Inc., USA) was used to carry out mass sequencing to generate sequencing data called reads. Mapping was accomplished by trimming reads to reference sequences based on human gene sequences. The mapping process may generate different reads depending on the experiment. Genes have different lengths, so mapping may vary in extent. Accordingly, the resulting values were derived after normalization, a calibration process, using EdgeR.

2.4 Differential gene expression analysis

mRNA-Seq reads were aligned with Bowtie2 (Langmead and Salzberg, 2012). Based on the genome assembly sequence or representative transcription sequence aligned with genome and transcriptome, the Bowtie2 index is generated. Alignment files were used for detection of differential expression of genes. Differentially expressed genes (DEGs) were extracted using Bedtools (Quinlan AR, 2010). Genes were categorized based on searches in DAVID (http://david.ncifcrf.gov/) and Medline (http://www.ncbi.nlm.nih.gov) databases.

2.4.1 Gene ontology analysis

HGF and PDL cells were analyzed by gene ontology (GO). Genes that showed $\geq$2-fold increase or decrease in expression in fluoride adhesive films relative to the control, normalized data (log2) $\geq$4, and p-value ≤ 0.05 were filtered.

2.4.2 Gene set enrichment analysis (GSEA)

For gene set enrichment analysis (GSEA), the online GSEA 4.0.0. program (http://software.broadinstitute.org/gsea/index.jsp) was used to find hallmark pathways. The false discovery rate (FDR) was set at $q < 0.05$. DEGs of HGF and PDL cells were compared among the three groups. GSEA was performed on genes that showed commonly decreased or increased

expression or opposite results.

2.5 Statistical analysis

The experimental data were analyzed using SPSS version 20.0 (SPSS Inc., Chicago, IL, USA). All variables, except those for DEG analysis, were analyzed using one-way analysis of variance (ANOVA), followed by Tukey's test. Results with p-value < 0.05 were considered statistically significant.

3. Results

3.1 MTT assay

The effects of PF-PVA and F-PVA on HGF and PDL cells, among oral cell lines, were analyzed by MTT assay. In PF-PVA group, both PDL and HGF cells were 70% and 64% higher in cytotoxicity than the control group, respectively. The PF-PVA group showed higher cytotoxicity than the F-PVA group (PDL cells: 37% and HGF cells: 40%, Fig. 1).

3.2 Differential gene expression analysis

3.2.1 Gene ontology analysis

3.2.1.1 HGF cells

Genetic analysis of HGF cells showed changes in the expression of genes associated with aging, apoptosis, cell death, cell migration, DNA repair, immune response, neurogenesis and secretion of GO with both PF-PVA and F-PVA (Fig. 2).

For cell death GO, PF-PVA significantly increased the expression of three genes (*growth arrest and DNA damage protein 45A* (GADD45A), *growth arrest and DNA damage-inducible 45 beta* (GADD45B), *protein phosphatase 1 regulatory subunit 15A* (PPP1R15A)) among 893 associated genes ($p < 0.05$) (Fig. 3).

The F-PVA group had more genes whose expression was significantly decreased than the PF-PVA group (Fig. 2). When treated under the same conditions, 2 out of 893 genes (*mixed lineage kinase domain-like protein* (MLKL) and *neuron-specific gene family member 1* (NSG1)) had increased expression, while 4 out of 893 genes (*DNA fragmentation factor subunit beta* (DFFB), *critical assessment of protein structure prediction round 9* (CASP 9), *critical assessment of protein structure prediction round 8* (CASP 8) and *myeloid differentiation primary response 88* (MYD88)) demonstrated decreased expression.

A comparison of DEGs in HGF cells of three groups revealed changes in expression in 22 genes: 10 genes with commonly increased expression and 12 genes with commonly decreased expression. There was one contra-regulated gene in the comparison between control and fluoride adhesive films (Fig. 4).

3.2.1.2 PDL cells

PDL cells were analyzed using the same method as HGF cells. In PDL cells of the PF-PVA, more genes showed changes

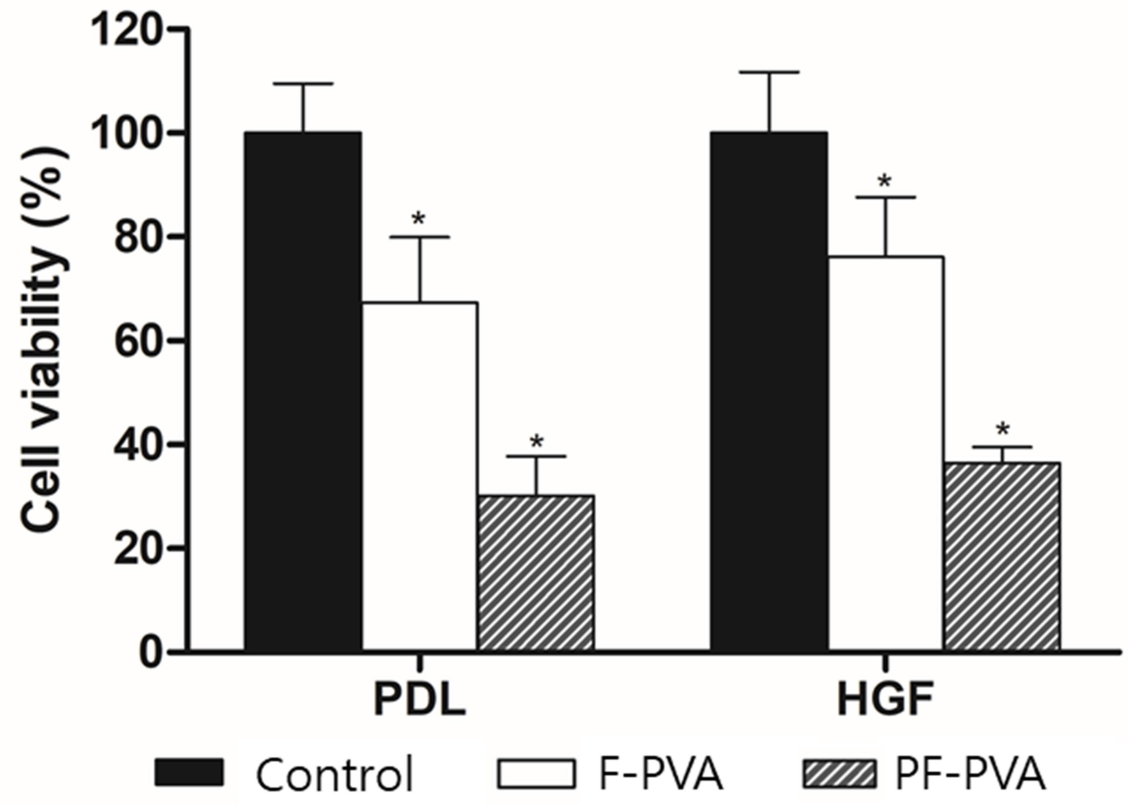

FIGURE 1. Cell viability evaluated by MTT assay. Cytotoxicity of control, NaF-PVA tape, and pullulan + NaF-PVA tape was investigated in human PDL and HGF cell lines. Data represent the mean and standard deviation of 3 independent experiments. One-way analysis of variance (ANOVA) followed by Tukey's test (*: $p < 0.05$). PDL: periodontal ligament; HGF: human gingival fibroblast; F-PVA: fluoride-polyvinyl alcohol; PF-PVA: pullulan-incorporated F-PVA.

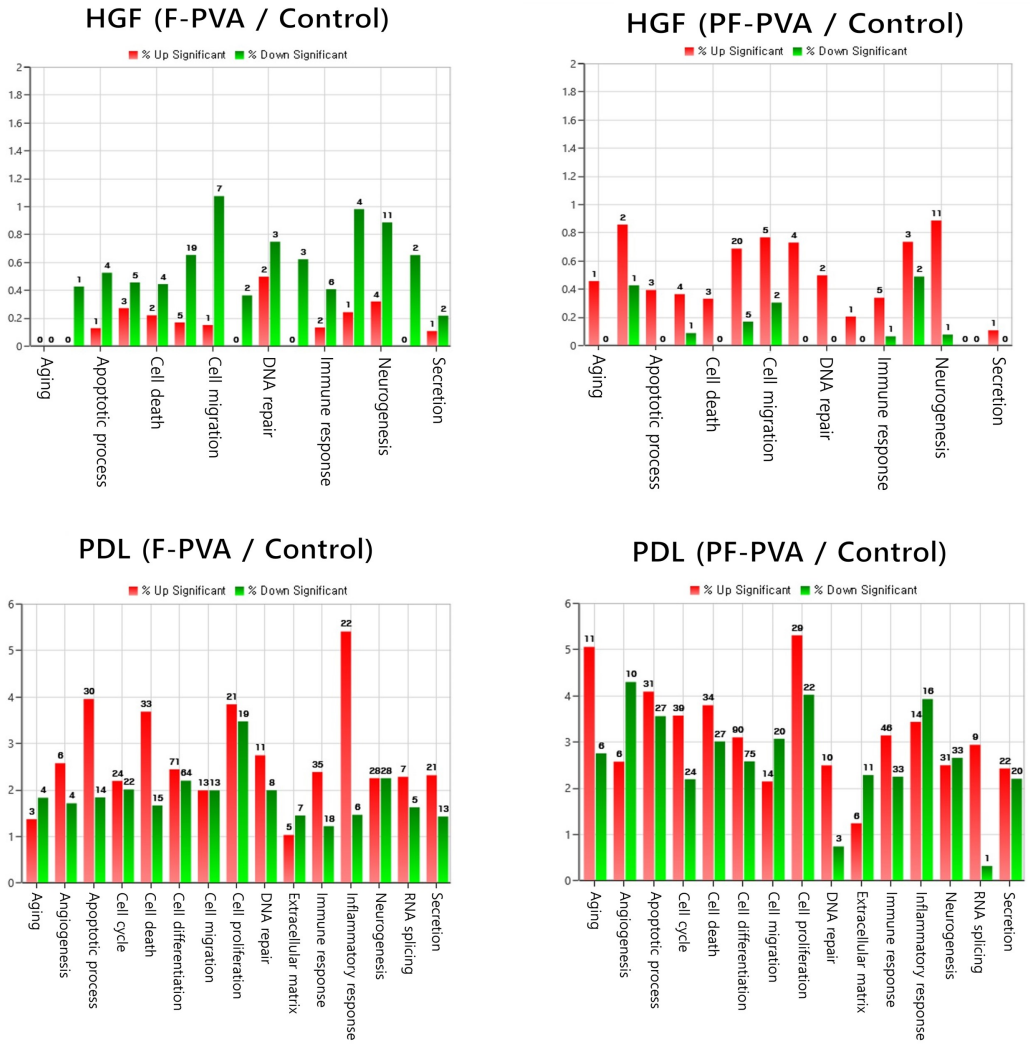

FIGURE 2. Gene category chart of human gingival fibroblast (HGF) and periodontal ligament (PDL) cells. Overview of differentially expressed genes (DEGs) in PF-PVA and F-PVA compared to control. F-PVA: fluoride-polyvinyl alcohol; PF-PVA: pullulan-incorporated F-PVA; HGF: human gingival fibroblasts; PDL: human periodontal ligament.

in expression s than HGF cells in DEGs analysis. There were 34 over-expressed genes and 27 under-expressed genes among 893 genes associated with cell death GO based on the changes in gene expression by GO. DEG analysis of F-PVA revealed 33 over-expressed genes and 15 under-expressed genes, indicating that more genes were affected by changes in expression than in HGF cells. In contrast to PF-PVA, fewer genes showed changes (Figs. 2,3).

DEGs in three different groups of PDL cells were compared, revealing the same pattern of change in expression among a total of 317 genes: 177 genes with commonly increased expression and 140 genes with commonly decreased expression. Unlike HGF cells, there were 33 contra-regulated genes among fluoride adhesive films, compared to the control (Fig. 4).

3.2.2 Gene set enrichment analysis (GSEA)

3.2.2.1 HGF cells

When the hallmark pathway method was applied, only one key pathway (TNFA_SIGNALING_VIA_NFκB) was derived from the PF-PVA (Table 1). Fig. 5 shows the genes that influence the hallmark key pathway.

In the F-PVA group, GSEA results showed no hallmark key pathway. In the absence of a key pathway, genes influencing such pathways could not be derived. The results of GSEA on 22 genes that showed changes in expression in both PF-PVA and F-PVA groups indicated no hallmark key pathway.

Based on these findings, HGF cells showed changes in expression occurring in a greater number of genes when pullulan was added to fluoride adhesive films. In contrast, conventional fluoride adhesive films did not show significant gene mutations.

3.2.2.2 DL cells

Based on the hallmark pathway method, Tables 2,3,4 describe the key pathways for changes in gene expression in PDL cells. GSEA results on gene expression changes in PF-PVA, F-PVA and both groups identified at least five key pathways and only five key pathways with the highest significance were described. With HGF cells, the key pathway with the highest significance was TNFA_SIGNALING_VIA_NFκB in all groups.

Genes that influenced hallmark key pathways are described in Tables 2,3,4 and their names are illustrated (Fig. 6). Among

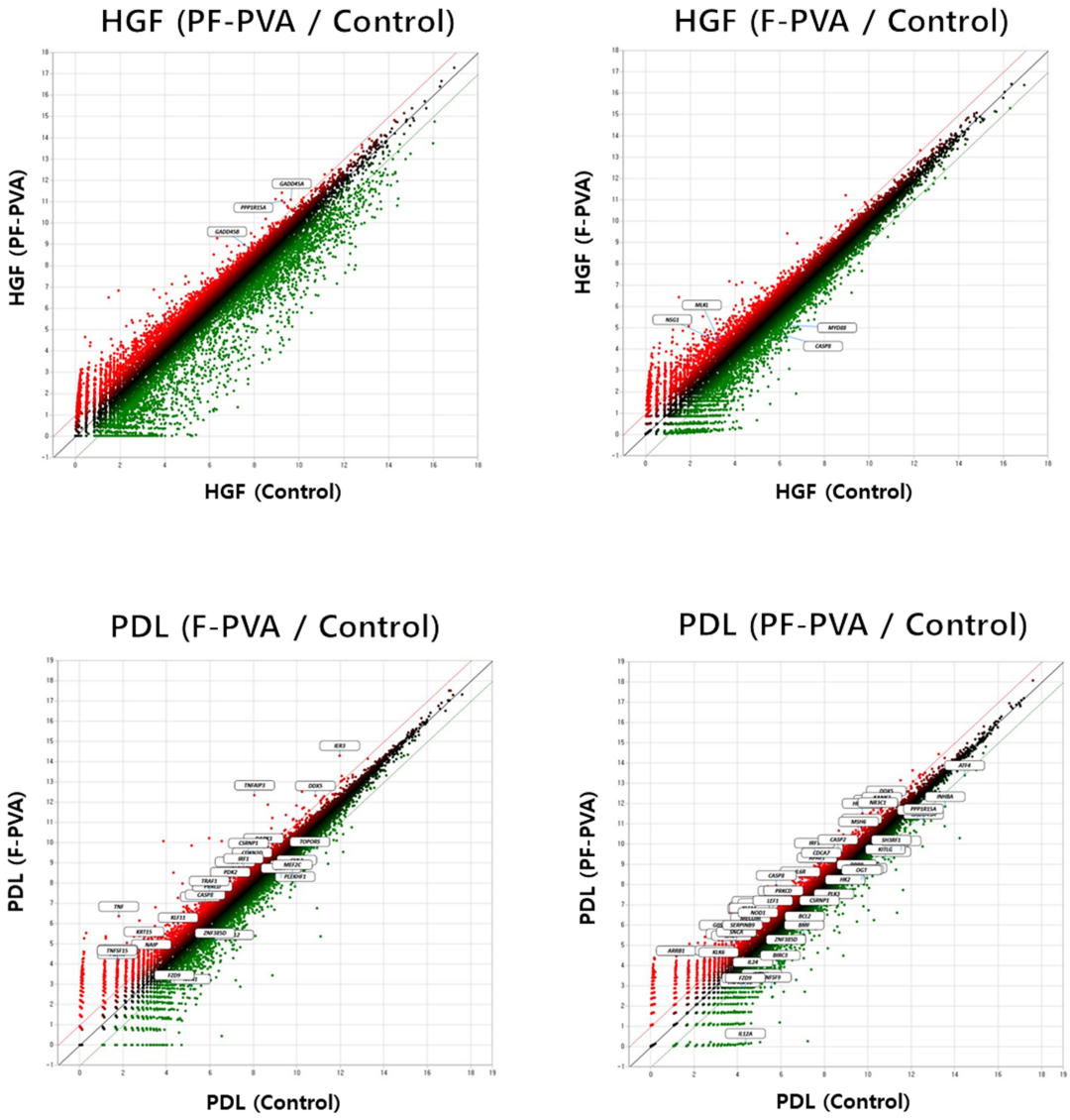

FIGURE 3. Scatter plots of gene expression. In each plot, the central line indicates no difference in expression between cells (groups). Genes named in the square box are gene associated with cell death gene ontology (GO). A red plot presents upregulated genes and a green plot presents downregulated genes. x-axis: normalized data (log2) of control group, y-axis: normalized data (log2) of experimental group. F-PVA: fluoride-polyvinyl alcohol; PF-PVA: pullulan-incorporated F-PVA; HGF: human gingival fibroblasts; PDL: human periodontal ligament.

TABLE 1. Gene set enrichment analysis (GSEA) of differentially expressed genes (DEGs) on human gingival fibroblast (HGF) cells in PF-PVA.

Gene set name	Description	Genes in overlap	*p*-value	FDR *q*-value
HALLMARK_TNFA_SIGNALIN _VIA_NFKB	Genes regulated by NF-κB in response to TNF	15	2.06×10^{-17}	1.03×10^{-15}

Only gene sets with p-value < 0.05 were included.
FDR: false discovery rate; TNF: tumor necrosis factor; NF-κB: nuclear factor kappa-light-chain-enhancer of activated B cells.

the genes that influenced key pathways, only 15 were selected and displayed in Fig. 6.

4. Discussion

Recent studies in medicine have examined drug releasing technology and technologies for controlling and regulating drug diffusion rates and their rate of reaching target organs [18–20]. Various forms of mucoadhesion products have been developed to extend drug residence times. Based on a similar concept, fluoride adhesive films have been developed to control the fluoride release rate in films affixed to teeth [21].

Nanotechnology can create materials or devices with new properties and functions by manipulating ultrafine materials on the atomic or molecular level [22]. Nano-type fluoride shows greater response due to better solubility than macro-

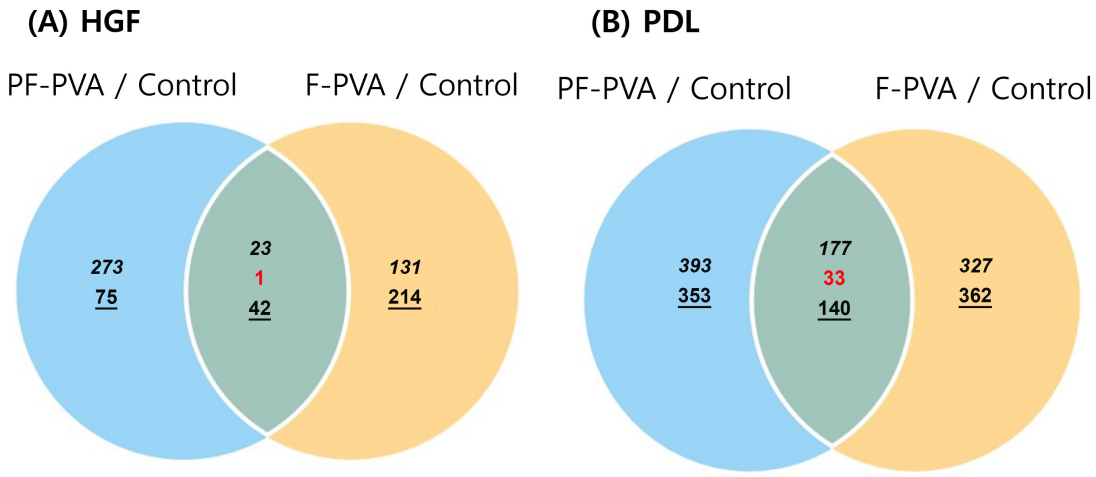

FIGURE 4. Gene set enrichment analysis, Venn diagram. (A) HGF cells, (B) PDL cells. Slanted numbers: number of up-regulated genes, red numbers: number of contra-regulated genes, underlined numbers: number of down-regulated genes. HGF: human gingival fibroblasts; PDL: human periodontal ligament.

Entrez Gene Id	Gene Symbol	HALLMARK_TNFA_SIGNALING_VIA_NFKB	Entrez	Ensembl	Gene Description
3949	LDLR				low density lipoprotein receptor [Source:HGNC Symbol;Acc:HGNC:6547]
2354	FOSB				FosB proto-oncogene, AP-1 transcription factor subunit [Source:HGNC Symbol;Acc:HGNC:3797]
2920	CXCL2				C-X-C motif chemokine ligand 2 [Source:HGNC Symbol;Acc:HGNC:4603]
4616	GADD45B				growth arrest and DNA damage inducible beta [Source:HGNC Symbol;Acc:HGNC:4096]
1647	GADD45A				growth arrest and DNA damage inducible alpha [Source:HGNC Symbol;Acc:HGNC:4095]
5743	PTGS2				prostaglandin-endoperoxide synthase 2 [Source:HGNC Symbol;Acc:HGNC:9605]
6347	CCL2				C-C motif chemokine ligand 2 [Source:HGNC Symbol;Acc:HGNC:10618]
6446	SGK1				serum/glucocorticoid regulated kinase 1 [Source:HGNC Symbol;Acc:HGNC:10810]
23645	PPP1R15A				protein phosphatase 1 regulatory subunit 15A [Source:HGNC Symbol;Acc:HGNC:14375]
79693	YRDC				yrdC N6-threonylcarbamoyltransferase domain containing [Source:HGNC Symbol;Acc:HGNC:28905]
2921	CXCL3				C-X-C motif chemokine ligand 3 [Source:HGNC Symbol;Acc:HGNC:4604]
1827	RCAN1				regulator of calcineurin 1 [Source:HGNC Symbol;Acc:HGNC:3040]
1958	EGR1				early growth response 1 [Source:HGNC Symbol;Acc:HGNC:3238]
23529	CLCF1				cardiotrophin like cytokine factor 1 [Source:HGNC Symbol;Acc:HGNC:17412]
8013	NR4A3				nuclear receptor subfamily 4 group A member 3 [Source:HGNC Symbol;Acc:HGNC:7982]
5999	RGS4				regulator of G protein signaling 4 [Source:HGNC Symbol;Acc:HGNC:10000]
29970	SCHIP1				schwannomin interacting protein 1 [Source:HGNC Symbol;Acc:HGNC:15678]
8817	FGF18				fibroblast growth factor 18 [Source:HGNC Symbol;Acc:HGNC:3674]
5833	PCYT2				phosphate cytidylyltransferase 2, ethanolamine [Source:HGNC Symbol;Acc:HGNC:8756]
8651	SOCS1				suppressor of cytokine signaling 1 [Source:HGNC Symbol;Acc:HGNC:19383]

FIGURE 5. Gene set overlap matrix prepared by gene set enrichment analysis (GSEA) on human gingival fibroblast (HGF) cells. GSEA was performed to identify the functional profiles of over-expressed genes in a large set and to identify the association between genes in the set. Hallmark gene set overlaps of cells were derived only from PF-PVA. Unmatched genes are hidden.

type fluoride [23]. For fluoride adhesive films, NaF was added through nanofiber spraying. Not only was this done to enhance the film's performance as a medium, but also to adjust its viscosity, elasticity, strength, adhesive force and surface tension. Fluoride adhesive film supplemented with pullulan was designed to take advantage of its easy composition change. The bio-stability of these two types of film was tested. MTT assay was performed on HGF and PDL cells to test fluoride

TABLE 2. Gene set enrichment analysis (GSEA) of differentially expressed genes (DEGs) on human periodontal ligament (PDL) cells in PF-PVA.

Gene set name	Description	Genes in overlap	*p*-value	FDR *q*-value
HALLMARK_TNFA_SIGNALING_VIA_NFκB	Genes regulated by NF-κB in response to TNF	15	2.67×10^{-37}	1.34×10^{-35}
HALLMARK_INTERFERON_GAMMA_RESPONSE	Genes up-regulated in response to IFNG	26	3.22×10^{-11}	8.05×10^{-10}
HALLMARK_INFLAMMATORY_RESPONSE	Genes defining inflammatory response	23	4.89×10^{-9}	8.15×10^{-8}
HALLMARK_P53_PATHWAY	Genes involved in p53 pathways and networks	22	2.37×10^{-8}	2.97×10^{-7}
HALLMARK_APOPTOSIS	Genes mediating programmed cell death by activation of caspases	18	3.43×10^{-7}	3.43×10^{-6}

Only five key pathways with low p-value were included.
FDR: false discovery rate; TNF: tumor necrosis factor; NF-κB: nuclear factor kappa-light-chain-enhancer of activated B cells; IFNG: Interferon gamma.

TABLE 3. Gene set enrichment analysis (GSEA) of differentially expressed genes (DEGs) on human periodontal ligament (PDL) cells in F-PVA.

Gene set name	Description	Genes in overlap	*p*-value	FDR *q*-value
HALLMARK_TNFA_SIGNALING_VIA_NFκB	Genes regulated by NF-κB in response to TNF	47	4.78×10^{-32}	2.39×10^{-30}
HALLMARK_INFLAMMATORY_RESPONSE	Genes defining inflammatory response	23	1.24×10^{-9}	3.11×10^{-8}
HALLMARK_HYPOXIA	Genes up-regulated in response to low oxygen levels (hypoxia)	21	3.24×10^{-8}	5.4×10^{-7}
HALLMARK_P53_PATHWAY	Genes involved in p53 pathways and networks	19	6.68×10^{-7}	8.57×10^{-6}
HALLMARK_IL6_JAK_STAT3_SIGNALING	Genes up-regulated by IL6 via STAT3	12	1.62×10^{-6}	1.62×10^{-5}

Only five key pathways with low p-value were included.
FDR: false discovery rate; NF-κB: nuclear factor kappa-light-chain-enhancer of activated B cells; TNF: tumor necrosis factor; IL6: interleukin 6; STAT3: signal transducer and activator of transcription 3.

TABLE 4. Gene set enrichment analysis (GSEA) of differentially expressed genes (DEGs) on human periodontal ligament (PDL) cells in PF-PVA and F-PVA.

Gene set name	Description	Genes in overlap	*p*-value	FDR *q*-value
HALLMARK_TNFA_SIGNALING_VIA_NFκB	Genes regulated by NF-κB in response to TNF	10	6.4×10^{-16}	3.2×10^{-14}
HALLMARK_INFLAMMATORY_RESPONSE	Genes defining inflammatory response	6	1.42×10^{-8}	3.55×10^{-7}
HALLMARK_P53_PATHWAY	Genes involved in p53 pathways and networks	5	6.24×10^{-7}	1.01×10^{-5}
HALLMARK_IL6_JAK_STAT3_SIGNALING	Genes up-regulated by IL6 via STAT3	4	8.08×10^{-7}	1.01×10^{-5}
HALLMARK_APOPTOSIS	Genes mediating programmed cell death by activation of caspases	4	9.38×10^{-6}	9.38×10^{-5}

Only five key pathways with low p-value were included.
FDR: false discovery rate. NF-κB: nuclear factor kappa-light-chain-enhancer of activated B cells; TNF: tumor necrosis factor; IL6: interleukin 6; STAT3: signal transducer and activator of transcription 3.

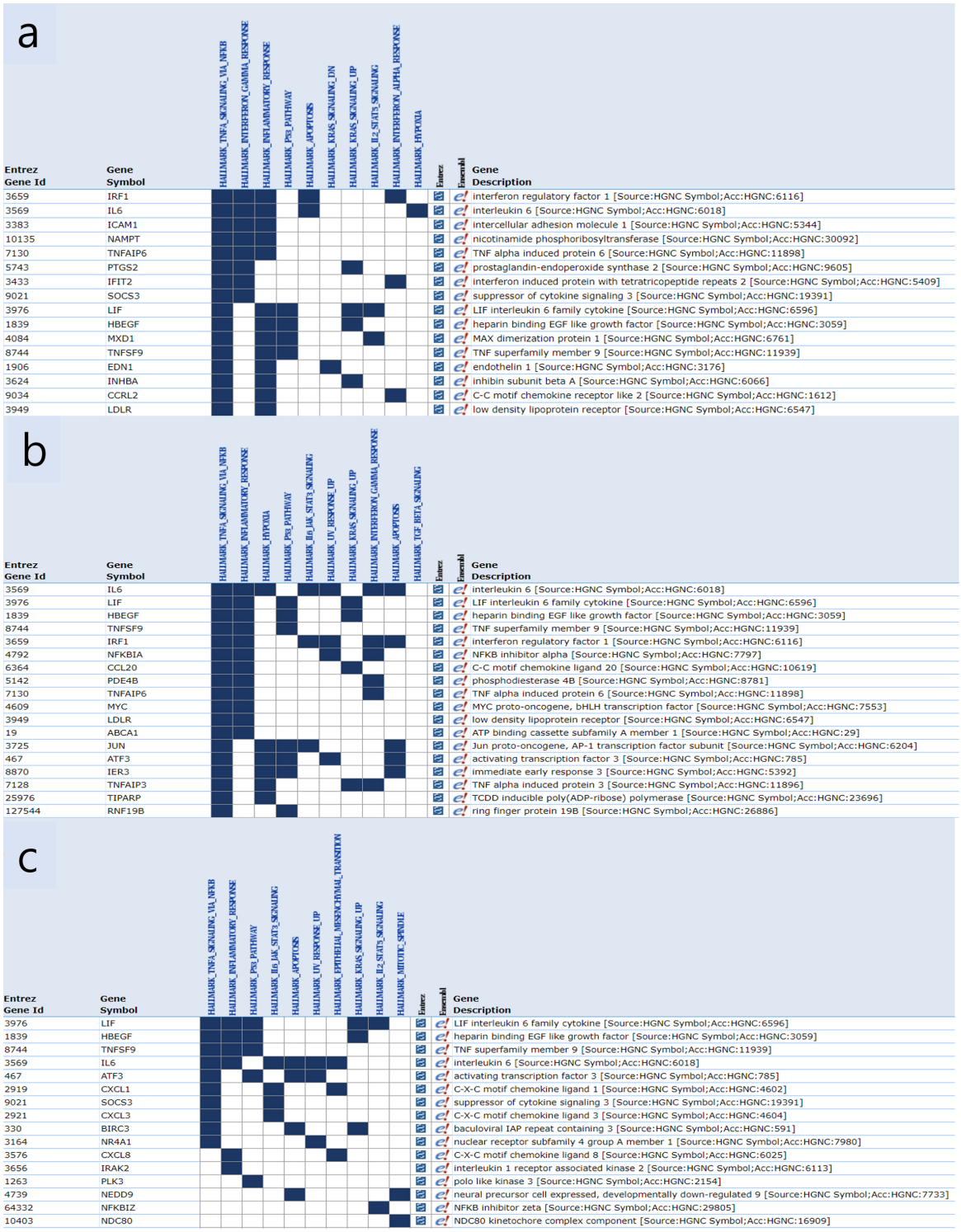

FIGURE 6. Gene set overlap matrix prepared by gene set enrichment analysis (GSEA) on human pediodontal ligament (PDL) cells. GSEA was performed to identify the functional profiles of over-expressed genes in a large set and to identify the association between genes in the set. Hallmark gene set overlaps of cells derived from PF-PVA (a), F-PVA (b) and both tapes (c). Only 15 genes were designated.

adhesive films' bio-stability. HGF and PDL cells were selected because fluoride adhesive films may have contact with enamel, gingiva and periodontal ligaments since they are applied to maxillary and mandibular arch units [7]. Despite the small possibility of direct contact between the fluorine adhesive film and PDL, experiments were conducted with both HGF and PDL cells to ensure the maximum safety of the product [24–26]. PF-PVA showed higher cytotoxicity than F-PVA in both cells. In HGF, F-PVA was considered non-cytotoxic as cell viability was not reduced by more than 30% compared to control. PF-PVA showed higher cytotoxicity compared to previous studies despite the fact that it showed lower antibacterial activity, contrary to our assumptions.

MTT assay is a simple and relatively accurate method for

assessing changes in cell proliferation and apoptosis, while enabling simultaneous measurement of large quantities [27]. However, to dissolve non-water-soluble formazan, organic solvents are needed. It is also possible to damage cells when removing the medium. Activities may differ depending on the physiological conditions of a single cell or cell type [28]. A major limitation of the MTT assay is that it can only assess cell viability binarily. Therefore, apoptosis cannot be clearly determined by this method alone [28, 29]. Moreover, genetic analysis was performed to overcome this problem, and to examine the causes of necroptosis and to observe the conditions of cells that come into contact with fluoride adhesive films in diverse manners [30].

RNA sequencing was performed on HGF and PDL cells applied to fluoride adhesive films to identify and analyze DEGs. All genetic analyses were conducted with the same parameters as previous genetic experiments used: fold value of 2, normalized data log value of $\geq$4, and p-value of ≤ 0.05 [31, 32].

Genes should be analyzed and grouped by function instead of independently since RNA sequencing involves tens of thousands of genes. GO is often used for this purpose [33–35]. It is a major bioinformatic initiative to unify gene attributes representation across all species. Genes with similar functions could be grouped as GO.

Gene category chart was used to identify which genes in what type of GO showed relatively greater changes in expression (Fig. 2). Cell aging or apoptosis may be associated with many types of GO. We observed changes in gene expression associated with aging, apoptotic process, cell death, cell migration, DNA repair, immune response, neurogenesis and secretion GO in HGF and PDL cells with both F-PVA and PF-PVA. Among the genes of cell death GO, which is considered to have the highest intuitive association with cytotoxicity among GOs, we examined genes that showed significant changes in expression.

When PF-PVA was applied, expression of the GADD45A, GADD45B and PPP1R15A genes increased in HGF cells. DNA repair, cell arrest and apoptosis are regulated by the GADD45 A and B genes. The GADD family protein PPP1R15A is also involved in apoptosis as it induces growth arrest and DNA damage [36, 37].

The MLKL and NSG1 genes were significantly upregulated when F-PVA was applied to HGF cells, while DFFB, CASP9, CASP8 and MYD88 genes were downregulated. The MLKL gene plays an important role in tumor necrosis factor (TNF) induced necroptosis [38, 39]. DNA damage also induces apoptosis through the NSG1 gene [40, 41]. While an increase in the expression of these genes contributed to cell death, the expression of other genes decreased, including the DFFB gene that induces chromatin condensation during apoptosis [42]; the CASP8/9 genes, a caspase family member also involved in apoptosis [43]; and the MYD88 gene [44]. Such results showed differences from fluoride adhesive films supplemented with pullulan.

It was found that PDL cells showed significantly more cell death GO expression changes than HGF cells. PF-PVA showed significant expression changes in 61 genes. Forty-eight in F-PVA, showing fewer genes with expression changes than in PF-PVA.

A clear conclusion cannot be reached on cytotoxicity based only on the number of genes from the results of analyzing changes in expression of various genes. However, a greater number of genes associated with cell death GO showed changes in expression with fluoride adhesive film supplemented with pullulan than conventional F-PVA. As a consequence, cell viability was affected. MTT assay results indicate this (Fig. 1).

Comparing DEGs of cells in the three groups using Venn diagrams, only PDL cells had contra-expressed genes between fluoride adhesive films, compared to the control (n = 33). Based on such findings, PDL cells are susceptible to more diverse changes than HGF cells depending on the type of fluoride adhesive film used.

DEG analysis requires significant effort to understand the reasons behind gene expression changes. Unless target genes are clearly defined, such efforts are likely to cause errors. Therefore, it is more efficient to find and analyze key pathways of genes [31, 45, 46]. GSEA is a program for analyzing significant gene sets in control and experimental groups using microarray or RNA-seq data. GSEA analyzes only human and mouse genes and is based on gene sets in the molecular signature database (MsigDB) [47–49]. Among the various methods available for identifying key pathways, the hallmark pathway method was used in this study [31].

When PF-PVA was applied, GSEA results showed that TNFA_SIGNALING_VIA_NFKB is the key pathway in HGF cells. Nuclear factor kappa-light-chain-enhancer of activated B cells (NF-κB) is a protein family involved in regulation of inflammatory response and immune system; necroptosis; cell proliferation; and differentiation of epithelial cells [50, 51]. TNF-α induces sustained inflammation in the body and is linked to various inflammatory diseases, including rheumatoid arthritis [52]. As with the cytological response observed when pullulan is used as a component of fluoride adhesive films, it could be viewed as a regulatory process of TNF-α that follows the NF-κB pathway. A possible mechanism by which PF-PVA could cause an inflammatory response in gingiva appears to involve influencing TNF-α through NF-κB in HGF cells. Based on this key pathway, the application of PF-PVA reduced cell viability by triggering an inflammatory response caused by the film.

As mentioned earlier, GSEA was performed to identify functional profiles of over-expressed genes in a large set and associations between genes in a set. From multiple genes, it was possible to examine each gene associated with the key pathway individually. On HGF cells, the NaF-PVA/Pullulan double layer adhesive film showed 15 genes involved in the key pathway (Fig. 5). Of these genes, LDLR gene deficiency increases plasma cholesterol levels and increased atherosclerosis risk. Increase in LDLR affects vascular inflammation [53]. The *chemokine* (*C-X-C motif*) *ligand 3* (CXCL3) gene is a gene of inflammation called macrophage inflammatory protein-2-β [54]. It could be deduced that TNF-α function was enhanced by expression changes in these 15 genes.

Comparing conventional fluoride adhesive film with control, GSEA results on HGF cells revealed no hallmark key pathway. In other words, GSEA based on genetic testing

produced results that supported MTT assay results.

GSEA results on PDL cells identified at least five key pathways from genes that showed changes in expression in PF-PVA, F-PVA and both groups. TNFA_SIGNALING_VIA_NFKB was the key pathway in all GSEAs. F-PVA also showed very high significance for this key pathway, but PF-PVA showed even higher significance.

To improve the adhesive force of conventional fluoride adhesive films, double layer adhesive films containing pullulan and PVA of different solubility properties were developed and showed higher cytotoxicity than conventional fluoride adhesive films. The DEG analysis results also indicate that the bio-stability of PDL cells is more vulnerable than HGF cells for all fluoride adhesive films. In children, fluoride adhesive films should only come into direct contact with the periodontal ligament in a few cases. However, several factors to consider when applying fluoride adhesive films to children: exposed roots due to abnormal mastication, gingival recession due to orthodontic treatment, exposed periodontal ligaments due to trauma, and significant alveolar bone resorption due to a systemic disease [55, 56]. Furthermore, the size of the fluoride adhesive film should be considered to minimize gingival contact and fabrication of customized fluoride adhesive films should enhance product safety.

Pullulan has structural flexibility with a uniform and unique linkage pattern of hydroxyl groups on glucopyranose rings. In contrast to other polysaccharides, it possesses distinct film-forming and fiber-forming properties [57]. Consequently, it is widely used in drug delivery, gene delivery, plasma expanders, tissue engineering, wound healing and oral care products [57, 58]. It is difficult to assume that the pullulan layer causes cytotoxicity based on its components and characteristics. It is believed that low cell viability would be difficult to verify by separate analyses of fluoride adhesive film and pullulan. Further studies on the interactions between pullulan and fluoride adhesive film are needed to determine the cause of such effects. Additionally, conducting further comparative studies on films with varying pullulan ratios could provide valuable insights and substantiate these findings.

It is true that pullulan can increase the adhesion of the film, but its disadvantages are evident from the increased cytotoxicity of the film in this experiment. Therefore, it is not recommended as a replacement for traditional F-PAV. Further studies on improving the application method of pullulan or materials that can replace pullulan are needed to improve fluoride adhesive films' stability.

5. Conclusions

In conclusion, this study confirmed PF-PVA exhibited high cytotoxicity in MTT assay and gene analysis using HGF and PDL cells. These results suggest that PF-PVA has lower biocompatibility levels than F-PVA.

AVAILABILITY OF DATA AND MATERIALS

The data presented in this study are available on reasonable request from the corresponding author.

AUTHOR CONTRIBUTIONS

YKC and MKJ—designed the research study; wrote the manuscript. OHN, SRJ and MKJ—performed the research. JHS and TYP—provided help and advice on the research. All authors contributed to editorial changes in the manuscript. All authors read and approved the final manuscript.

ETHICS APPROVAL AND CONSENT TO PARTICIPATE

The study was conducted following the Declaration of Helsinki. The study protocol was reviewed and approved by the Institutional Review Board of the Chosun University Dental Hospital, Seoul, Korea (CUDHIRB 2102-002).

ACKNOWLEDGMENT

Not applicable.

FUNDING

This study was supported by research fund from Chosun University Dental Hospital, 2024.

CONFLICT OF INTEREST

The authors declare no conflict of interest.

REFERENCES

[1] Dayo AF, Wolff MS, Syed AZ, Mupparapu M. Radiology of dental caries. Dental Clinics of North America. 2021; 65: 427–445.

[2] Featherstone JDB, Crystal YO, Alston P, Chaffee BW, Doméjean S, Rechmann P, *et al.* Evidence-based caries management for all ages-practical guidelines. Frontiers in Oral Health. 2021; 2: 657518.

[3] de Oliveira PRA, Barreto LSDC, Tostes MA. Effectiveness of CPP-ACP and fluoride products in tooth remineralization. International Journal of Dental Hygiene. 2022; 20: 635–642.

[4] Zhang Q, Guan L, Guo J, Chuan A, Tong J, Ban J, *et al.* Application of fluoride disturbs plaque microecology and promotes remineralization of enamel initial caries. Journal of Oral Microbiology. 2022; 14: 2105022.

[5] Schiffner U. Use of fluorides for caries prevention. Bundesgesundheitsblatt Gesundheitsforschung Gesundheitsschutz. 2021; 64: 830–837. (In German)

[6] Knutson JW. Sodium fluoride solutions: technic for application to the teeth. The Journal of the American Dental Association. 1948; 36: 37–39.

[7] Zendron MP, Rocha ADO, Simões MSDS, Santana CM, Bolan M, Cardoso M. Fluoride varnish in dentistry: a bibliometric analysis of the 100 most-cited papers. Caries Research. 2023; 57: 189–196.

[8] Noble J. Fluoride varnish for the teeth. Vital. 2008; 5: 39.

[9] Benedito LCB, Pedro Ricomini-Filho A, Tabchoury CPM, Cury JA. Anticaries potential of a fluoride foam. Brazilian Dental Journal. 2023; 34: 89–98.

[10] Mascarenhas AK. Is fluoride varnish safe? The Journal of the American Dental Association. 2021; 152: 364–368.

[11] Sousa GP, Lima CCB, Braga MM, Moura L, Lima MDM, Moura MS. Early childhood caries management using fluoride varnish and neutral fluoride gel: a randomized clinical trial. Brazilian Oral Research. 2022; 36: e099.

[12] Kim MJ, Lee SH, Lee NY, Lee IH. Evaluation of the effect of PVA tape supplemented with 2.26% fluoride on enamel demineralization using microhardness assessment and scanning electron microscopy: *in vitro* study. Archives of Oral Biology. 2013; 58: 160–166.

[13] Lee KY LS, Lee NY. Evaluation of fluoride-relasing capacity from polyvinyl alcohol polymer tape supplemented with NaF in oral cavity. Journal of the Korean Academy of Pediatric Dentistry. 2013; 40: 89–97.

[14] Jih MK, Lee SH, Lee NY. Physical and chemical properties of double-layers adhesive polymer film supplemented with 5% NaF. The Jounal of the Korean Dental Association. 2021; 59: 204–212.

[15] Jih M, Lee S, Lee N. Effect of polymer adhesive film supplemented 5% NaF on enamel remineralization. The Journal of the Korean Academy of Pedtatric Dentistry. 2014; 41: 218–224.

[16] Lee SH, Lee NY, Lee IH. Clinical evaluation of the efficacy of fluoride adhesive tape (F-PVA) in reducing dentin hypersensitivity. The American Journal of Dentistry. 2013; 26: 143–148.

[17] Oh YJ, Hong J. Application of the MTT-based colorimetric method for evaluating bacterial growth using different solvent systems. Lebensmittel-Wissenschaft & Technologie. 2022; 153: 112565.

[18] Li S, Zhang H, Chen K, Jin M, Vu SH, Jung S, *et al*. Application of chitosan/alginate nanoparticle in oral drug delivery systems: prospects and challenges. Drug Delivery. 2022; 29: 1142–1149.

[19] Singh RS, Kaur N, Singh D, Purewal SS, Kennedy JF. Pullulan in pharmaceutical and cosmeceutical formulations: a review. International Journal of Biological Macromolecules. 2023; 231: 123353.

[20] Suharyani I, Fouad Abdelwahab Mohammed A, Muchtaridi M, Wathoni N, Abdassah M. Evolution of drug delivery systems for recurrent aphthous stomatitis. Drug Design, Development and Therapy. 2021; 15: 4071–4089.

[21] Park DY, Lee NY, Lee SH. Preventive effect of fluoride-containing adhesive film made by nano technology on dental caries. Journal of the Korean Academy of Pediatric Dentistry. 2008; 35: 272662–272670.

[22] Netalkar PP, Sr M, Ym K, Natarajan S, Gadipelly T, Bhat P D, *et al*. Effect of nano-hydroxyapatite incorporation on fluoride-releasing ability, penetration, and adaptation of a pit and fissure sealant. International Journal of Paediatric Dentistry. 2022; 32: 344–351.

[23] Sun L, Chow LC. Preparation and properties of nano-sized calcium fluoride for dental applications. Dental Materials. 2008; 24: 111–116.

[24] Gamal AY, Bayomy MM. Effect of cigarette smoking on human PDL fibroblasts attachment to periodontally involved root surfaces *in vitro*. Journal of Clinical Periodontology. 2002; 29: 763–770.

[25] Holliday RS, Campbell J, Preshaw PM. Effect of nicotine on human gingival, periodontal ligament and oral epithelial cells. A systematic review of the literature. Journal of Dentistry. 2019; 86: 81–88.

[26] Lai YL, Chen YT, Lee SY, Shieh TM, Hung SL. Cytotoxic effects of dental resin liquids on primary gingival fibroblasts and periodontal ligament cells *in vitro*. Journal of Oral Rehabilitation. 2004; 31: 1165–1172.

[27] Maru VP, Madkaikar M, Sattar S, Chauhan R, Devi RKS. Response of intra canal medicaments on viability and survival of SHEDs. Journal of Clinical Pediatric Dentistry. 2022; 46: 65–71.

[28] Angius F, Floris A. Liposomes and MTT cell viability assay: an incompatible affair. Toxicology in Vitro. 2015; 29: 314–319.

[29] Gomez Perez M, Fourcade L, Mateescu MA, Paquin J. Neutral red versus MTT assay of cell viability in the presence of copper compounds. Analytical Biochemistry. 2017; 535: 43–46.

[30] Maru V, Shetty O, Dixit U, Warke VG, Khande M, Mane S. SHED's response to various pulpotomy materials: cytotoxicity and gene expression analysis. Journal of Clinical Pediatric Dentistry. 2021; 45: 406–413.

[31] Nam OH, Oh TJ, Lee J, Hwang Y, Choi SC. Differential gene expression profiles of human periodontal ligament cells preserved in Hank's balanced salt solution and milk. Dental Traumatology. 2020; 36: 58–68.

[32] Rathinam E, Govindarajan S, Rajasekharan S, Declercq H, Elewaut D, De Coster P, *et al*. Transcriptomic profiling of human dental pulp cells treated with tricalcium silicate-based cements by RNA sequencing. Clinical Oral Investigations. 2021; 25: 3181–3195.

[33] Katsuda T. Sub-GOFA: a tool for Sub-Gene Ontology function analysis in clonal mosaicism using semantic (logical) similarity. Bioinformation. 2022; 18: 53–60.

[34] Tickotsky N, Moskovitz M. Protein activation in periapical reaction to iodoform containing root canal sealer. Journal of Clinical Pediatric Dentistry. 2017; 41: 450–455.

[35] Zhang C, Sun Y, Xu M, Shu C, Yue Z, Hou J, *et al.* Potential links between COVID-19 and periodontitis: a bioinformatic analysis based on GEO datasets. BMC Oral Health. 2022; 22: 520.

[36] Monkley S, Overed-Sayer C, Parfrey H, Rassl D, Crowther D, Escudero-Ibarz L, *et al.* Sensitization of the UPR by loss of PPP1R15A promotes fibrosis and senescence in IPF. Scientific Reports. 2021; 11: 21584.

[37] Song Y, Liu S, Zhao Z, Zhang Y, Yang Y, Luo B. Relationship between PPP1R15A gene polymorphism (rs611251) and Epstein-Barr virus-associated tumors. Acta Virologica. 2017; 61: 445–452.

[38] Dovey CM, Diep J, Clarke BP, Hale AT, McNamara DE, Guo H, *et al.* MLKL requires the inositol phosphate code to execute necroptosis. Molecular Cell. 2018; 70: 936–948.e937.

[39] zhong Y, Zhang ZH, Wang JY, Xing Y, Ri MH, Jin HL, *et al*. Zinc finger protein 91 mediates necroptosis by initiating RIPK1-RIPK3-MLKL signal transduction in response to TNF receptor 1 ligation. Toxicology Letters. 2022; 356: 75–88.

[40] Sun G, Zhao T. Lung adenocarcinoma pathology stages related gene identification. Mathematical Biosciences and Engineering. 2020; 17: 737–746.

[41] Yap CC, Digilio L, McMahon L, Winckler B. The endosomal neuronal proteins Nsg1/NEEP21 and Nsg2/P19 are itinerant, not resident proteins of dendritic endosomes. Scientific Reports. 2017; 7: 10481.

[42] Bi H, Wang G, Li Z, Zhou L, Zhang M. MEG3 regulates CSE-induced apoptosis by regulating miR-421/DFFB signal axis. International Journal of Chronic Obstructive Pulmonary Disease. 2023; 18: 859–870.

[43] Ma T, Li H, Liu H, Peng Y, Lin T, Deng Z, *et al*. Neat1 promotes acute kidney injury to chronic kidney disease by facilitating tubular epithelial cells apoptosis via sequestering miR-129-5p. Molecular Therapy. 2022; 30: 3313–3332.

[44] Zhu Y, Han Q, Wang L, Wang B, Chen J, Cai B, *et al*. Jinhua Qinggan granules attenuates acute lung injury by promotion of neutrophil apoptosis and inhibition of TLR4/MyD88/NF-κB pathway. Journal of Ethnopharmacology. 2023; 301: 115763.

[45] Dai Y, Sun X, Wang C, Li F, Zhang S, Zhang H, *et al*. Gene co-expression network analysis reveals key pathways and hub genes in Chinese cabbage (Brassica rapa L.) during vernalization. BMC Genomics. 2021; 22: 236.

[46] López-Otín C, Blasco MA, Partridge L, Serrano M, Kroemer G. The hallmarks of aging. Cell. 2013; 153: 1194–1217.

[47] Chovatiya G, Ghuwalewala S, Walter LD, Cosgrove BD, Tumbar T. High-resolution single-cell transcriptomics reveals heterogeneity of self-renewing hair follicle stem cells. Experimental Dermatology. 2021; 30: 457–471.

[48] Fan J, Shi S, Qiu Y, Liu M, Shu Q. Analysis of signature genes and association with immune cells infiltration in pediatric septic shock. Frontiers in Immunology. 2022; 13: 1056750.

[49] Pistis G, Vázquez-Bourgon J, Fournier M, Jenni R, Cleusix M, Papiol S, *et al*. Gene set enrichment analysis of pathophysiological pathways highlights oxidative stress in psychosis. Molecular Psychiatry. 2022; 27: 5135–5143.

[50] Capece D, Verzella D, Flati I, Arboretto P, Cornice J, Franzoso G. NF-κB: blending metabolism, immunity, and inflammation. Trends in Immunology. 2022; 43: 757–775.

[51] DiDonato JA, Mercurio F, Karin M. NF-κB and the link between inflammation and cancer. Immunological Reviews. 2012; 246: 379–400.

[52] Lauper K, Iudici M, Mongin D, Bergstra SA, Choquette D, Codreanu C, *et al.* Effectiveness of TNF-inhibitors, abatacept, IL6-inhibitors and JAK-inhibitors in 31 846 patients with rheumatoid arthritis in 19 registers from the 'JAK-pot' collaboration. Annals of the Rheumatic Diseases. 2022; 81: 1358–1366.

[53] Go GW, Mani A. Low-density lipoprotein receptor (LDLR) family orchestrates cholesterol homeostasis. Yale Journal of Biology and Medicine. 2012; 85: 19–28.

[54] Kusuyama J, Komorizono A, Bandow K, Ohnishi T, Matsuguchi T. CXCL3 positively regulates adipogenic differentiation. Journal of Lipid Research. 2016; 57: 1806–1820.

[55] Bimstein E. Periodontal health and disease in children and adolescents. Pediatric Clinics of North America. 1991; 38: 1183–1207.

[56] Gebistorf M, Mijuskovic M, Pandis N, Fudalej PS, Katsaros C. Gingival recession in orthodontic patients 10 to 15 years posttreatment: a retrospective cohort study. American Journal of Orthodontics and Dentofacial Orthopedics. 2018; 153: 645–655.

[57] Singh RS, Kaur N, Rana V, Kennedy JF. Pullulan: a novel molecule for biomedical applications. Carbohydrate Polymers. 2017; 171: 102–121.
[58] Le NN, Le-Vinh B, Friedl JD, Jalil A, Kali G, Bernkop-Schnürch A. Polyaminated pullulan, a new biodegradable and cationic pullulan derivative for mucosal drug delivery. Carbohydrate Polymers. 2022; 282: 119143.

How to cite this article: Seo-Rin Jeong, Yong Kwon Chae, Ok Hyung Nam, Tae-Young Park, Jonghyun Shin, Myeong-Kwan Jih. Cytotoxicity of two fluoride-releasing adhesive tapes. Journal of Clinical Pediatric Dentistry. 2024; 48(5): 154-165. doi: 10.22514/jocpd.2024.115.